Brain-Specific Metallothionein-3 Has Higher Metal-Binding Capacity than Ubiquitous Metallothioneins and Binds Metals Noncooperatively †

ARTICLE *in* BIOCHEMISTRY · JUNE 2002

Impact Factor: 3.02 · DOI: 10.1021/bi025664v · Source: PubMed

6 AUTHORS, INCLUDING:

Peep Palumaa
Tallinn University of Technology
60 PUBLICATIONS **1,381** CITATIONS
SEE PROFILE

Elo Eriste
University of Tartu
27 PUBLICATIONS **764** CITATIONS
SEE PROFILE

Brain-Specific Metallothionein-3 Has Higher Metal-Binding Capacity than Ubiquitous Metallothioneins and Binds Metals Noncooperatively†

Peep Palumaa,*,‡,§ Elo Eriste,|| Olga Njunkova,‡ Lesja Pokras,‡ Hans Jörnvall,|| and Rannar Sillard||

Centre for Gene Technology, Tallinn Technical University, Ehitajate tee 5, EE-19086 Tallinn, Estonia, Department of Medical Biochemistry and Biophysics, Karolinska Institutet, SE-171 77 Stockholm, Sweden, and National Institute of Chemical Physics and Biophysics, Akadeemia tee 23, EE−12618 Tallinn, Estonia

Received February 11, 2002; Revised Manuscript Received March 26, 2002

ABSTRACT: Zinc metabolism in the cells is largely regulated by ubiquitous small proteins, metallothioneins (MT). Metallothionein-3 is specifically expressed in the brain and is down regulated in Alzheimer's disease. We demonstrate by mass spectrometry that MT-3, in contrast to common MTs, binds Zn^{2+} and Cd^{2+} in a noncooperative manner and can also bind higher stoichiometries of metals than seven. MT-3 reconstituted with seven metals exists in a dynamic equilibrium of different metalloforms, where the prevalent metalloform is Me_7MT-3, but metalloforms with 6, 8, and even 9 metals are also present. The results from pH and stability studies demonstrate that the heterogeneity of metalloforms originates from the N-terminal β-cluster, whereas the C-terminal α-cluster of MT-3 binds four metal ions such as that of common MTs. Experiments with EDTA demonstrate that the β-cluster of ZnMT-3 has a higher metal transfer potential than the β-cluster of Zn_7MT-2. Moreover, ZnMT-3 loses metals during ultrafiltration. MT-3, reconstituted with an excess of Zn^{2+} or Cd^{2+}, exists as a dynamic mixture of metalloforms with higher than 7 metal stoichiometries (8−11). Such forms of ZnMT-3 are unstable and decompose partly already during a rapid gel filtration, whereas CdMT-3 forms are more stable. Extra metal ions may bind to the β-cluster region as well as to the carboxylates of MT-3. The specific metal-binding properties of MT-3 could be functionally implemented for buffering of fluctuating concentrations of zinc in zincergic neurons and for transfer of zinc to synaptic vesicles.

Cellular zinc homeostasis is largely regulated by metallothioneins (MTs),[1] a class of small cysteine- and metal-rich proteins (*1*). Mammalian MTs consist of 60−68 amino acid residues with an absolutely conserved pattern of 20 cysteine residues (*2*), adapted for clustering of essential (Zn^{2+} and Cu^{+}) and toxic (Cd^{2+}, Hg^{2+}) transition-metal ions (*2*). Common MT isoforms, MT-1 and MT-2, composed of 61 or 62 amino acids, are expressed in almost all tissues and show high levels in the liver and kidney (*3*). Common MTs bind cooperatively seven Zn^{2+} or Cd^{2+} ions (*2*), and 3-D structures for this type of MT metalloforms have been resolved by NMR (*4*) and X-ray diffraction (*5*). All resolved structures are similar and display two domains, both folded into metal−thiolate clusters: the N-terminal β domain contains a cluster of three metals coordinated with nine thiolates and the C-terminal α domain contains a cluster of four metals coordinated with 11 thiolates (*6*).

MT-3, a brain-specific MT isoform, was discovered from the brain extracts of patients with Alzheimer's disease (AD) as a downregulated protein in which contrast to other MTs inhibits the growth of neurons and was therefore denoted as a growth inhibitory factor (GIF) (*7*). The primary structure of MT-3 has approximately 70% identity with MT-1/MT-2; however, MT-3 consists of 68 amino acid residues and has two additional inserts, a single amino acid insert (Thr) close to the N-terminus and a glutamate-rich hexapeptide insert close to the C-terminus of the protein (*7*). MT-3 differs from common MTs also in gene regulation (*8*, *9*), in transcriptional regulation during development (*10*), and in the phenotype of transgenic animals (*11*, *12*). All these facts suggest a specific role for MT-3 in the brain, which could be connected with inhibition of neuronal growth (*7*, *13*, *14*). However, the mechanism of MT-3 action is unknown, and as MT-3 is particularly abundant in glutamatergic neurons containing vesicular zinc, there are also suggestions that MT-3 participates in utilization of zinc as a neuromediator (*15*, *16*).

The specific functional properties of MT-3 should rely on a different structure or on particular metal-binding properties. Up to now, the general view is that MT-3 binds seven Zn^{2+} and Cd^{2+} ions, much like the common MTs (*14*, *17*−*20*) and that it has similar cluster stabilities (*14*, *19*). However, ^{113}Cd−NMR studies of CdMT-3 have demonstrated that the β-cluster region of MT-3, in contrast to that of common MTs,

† This work was supported by the Estonian Science Foundation Grant 4287, the Swedish Institute Visby Program, and Karolinska Institutet.

* Corresponding author. Phone: +372 6398379. Fax: +372 6202020. E-mail: peepp@staff.ttu.ee.

‡ Tallinn Technical University.

§ National Institute of Chemical Physics and Biophysics.

|| Department of Medical Biochemistry and Biophysics Karolinska Institutet.

[1] Abbreviations: MT, metallothionein; GIF, growth inhibitory factor; AD, Alzheimer's disease; Aβ, amyloid β; NMR, nuclear magnetic resonance; DTT, 1,4-dithiothreitol; ESI-TOF-MS, electrospray ionization time-of-flight mass spectrometry.

10.1021/bi025664v CCC: $22.00
Published on Web 04/20/2002

is conformationally dynamic (*19*, *20*). The same conclusion was drawn also from high-resolution NMR studies of CdMT-3, where due to the dynamic processes, the structure of the N-terminal region of MT-3 was not resolved while the C-terminal part of MT-3 was shown to fold into the four-metal cluster similar to the α domains of MT-1 and MT-2 (*18*). Observed dynamic phenomena are explained mainly by the fast equilibria between different conformers of the three-metal cluster of Cd_7MT-3 (*18*−*20*), but the exact reasons are unknown.

The present work was directed to detailed metal-binding studies of MT-3 by ESI-TOF-MS with the hope to uncover the molecular background for specific structural dynamics of MT-3, which may have functional importance. We can now demonstrate that the β domain of MT-3 is adapted for noncooperative binding of variable concentrations of Zn^{2+} or Cd^{2+} ions and exposes high metal exchange potential, which suggests that one of the specific functions of MT-3 could be buffering of highly fluctuating concentrations of zinc and transfer of zinc into zinc vesicles in the regions of zincergic neurons in the brain.

MATERIALS AND METHODS

Rabbit MT-1 and MT-2 isoforms were isolated from livers of cadmium-exposed rabbits (*21*), while apo-MT isoforms were purified to homogeneity by reversed-phase HPLC (*22*) using an YMC ODS-AP column, 10 × 100 mm (5 μm, 300 Å). Homogeneous apo-MT forms were lyophilised and used for reconstitution experiments.

cDNA of human MT-3, obtained from Professor R. Palmiter, University of Washington, was inserted into plasmid pET21 (Novagen, Darmstadt, Germany). Recombinant human MT-3 was expressed in *Escherichia coli* and purified according to a modified general procedure (*20*). ZnMT-3 was isolated by gel filtration on a Superdex 75 column (Amersham Bioscience, Uppsala, Sweden), and apo-MT-3 was purified by a two-step procedure. First, crude MT-3 was applied to an ion exchange column, Resource S (Amersham Bioscience), equilibrated with 20 mM sodium phosphate (pH 2.5) and 20% acetonitrile (eluent A). MT-3 was eluted with a gradient of 0−0.5 M NaCl in buffer A (eluent B) covering 30 column volumes (CV). The material in the peak fraction, eluting at 0.21 M NaCl, was collected and purified to homogeneity by reversed-phase HPLC on Vydac C18 22 × 250 mm column. Lyophilised homogeneous apo-MT-3 was used for reconstitution experiments. Chromatographic experiments were carried out on ÄKTA HPLC systems (Amersham Biosciences). The molecular masses and the purity of the products were determined by analysis of MS spectra recorded on an Ettan electrospray time-of-flight mass spectrometer (ESI-TOF-MS) (Amersham Biosciences).

Reconstitution of MT Metalloforms. We have conducted two types of reconstitution experiments. In the first type, various concentrations of metals were added to apo-MT-3 (final concentration 10 μM) in degassed 5 mM ammonium acetate buffer (pH 7.5), containing 25 μM DTT. Samples were injected directly into the mass spectrometer or desalted on MicroSpin G-25 columns (Amersham Bioscience) equilibrated with 5 mM ammonium acetate (pH 7.5) prior to MS analysis. In the second type of experiments, metal salts (cadmium acetate or zinc acetate) were added to apo-MT (MT-1A or apo-MT-2A 10 μM; MT-3-20 μM) in degassed 20 mM formic acid (pH 2.7), containing 25 μM DTT, and the pH of the solution was raised to pH 8.5 with appropriate amount of ammonia solution. Before MS analysis, the buffer was exchanged to 5 mM ammonium acetate with a different pH by using MicroSpin G-25 columns, and the eluate was injected directly into the MS instrument. NanoSpin centrifugal filters (Gelman Laboratory Ann Arbor, MI) with a MW cut off of 4 kD were used for ultrafiltration of samples.

RESULTS

Purification of MT Isoforms. The main isoform from the rabbit liver MT-1 fraction (MT-1A) eluted from the final reversed-phase HPLC column at 21.5% acetonitrile, while MT-2C and MT-2A from the MT-2 fraction eluted at 22.1% and 22.3% acetonitrile, respectively. MS analysis demonstrated that the purity of the products is higher than 90%, and the following molecular mass values were obtained: MT-1A, 6144.8; MT-2A, 6125.2; MT-2C, 6154.8, which correspond to N-terminally acetylated rabbit MT forms. Recombinant MT-3 eluted from a final reversed-phase HPLC column at 27.7−28.3% acetonitrile. MS analysis confirmed that the purity of MT-3 is higher than 95% and has a molecular mass of 6927.4, which corresponds to human MT-3 without N-terminal acetylation.

Reconstitution of MT-3 with Zn^{2+}. MS spectra of MT-3, reconstituted at pH 7.5 with increasing stoichiometries of Zn^{2+} ions, are presented in Figure 1. At all stoichiometries of added zinc, MT-3 exposes multiple metalloforms. Even MT-3 reconstituted with 7 Zn^{2+} equiv at pH 7.5 exposes three metalloforms, with stoichiometries of 6−8, where Zn_7-MT-3 is the most populated form. There are practically no differences in MS spectra of ZnMT-3 reconstituted with zinc at pH 7.5 and ZnMT-3 reconstituted by metals at low pH and then raised to neutrality. Natively isolated ZnMT-3 displays an MS spectrum containing a major Zn_7MT-3 form and minor Zn_6MT-3 and Zn_8MT-3 forms, similar to the MT-3 reconstituted with 6−7 Zn^{2+} ions. By addition of more than 7 equiv of zinc, the equilibrium shifts toward metalloforms with higher than 7 metal stoichiometries, and metalloforms of MT-3 with up to 12 bound metals could be observed in the MS spectra. The results indicate that MT-3 is not present as a single metalloform in solution but exists as a dynamic mixture of different metalloforms, where metal stoichiometry is also higher than 7.

Stability of Zn MT-3. We tested the stability of ZnMT-3 in fast gel filtration experiments, in extended ultrafiltration, by exposure to EDTA, and at different pH values (Figure 2). Results demonstrate that ZnMT-3 metalloforms with metal stoichiometries up to 7 are stable during rapid gel filtration. ZnMT-3 metalloforms with higher metal stoichiometries (8−11) are partly decomposed during the quick gel filtration, while metalloforms with metal stoichiometries 8 and 9 are more stable. Prolonged ultrafiltration can remove metals even from Zn_7MT-3 with formation of Zn_6MT-3 and Zn_5MT-3. By addition of 20 μM EDTA to 10 μM Zn_7MT-3, four metalloforms with metal stoichiometries of 4−7 were observed, demonstrating that EDTA at low concentrations extracts metals from Zn_7MT-3. The results of the pH studies demonstrate that ZnMT-3 at pH 5.0 exposes four forms with metal stoichiometries of 4−7 in which the Zn_4MT-3 form

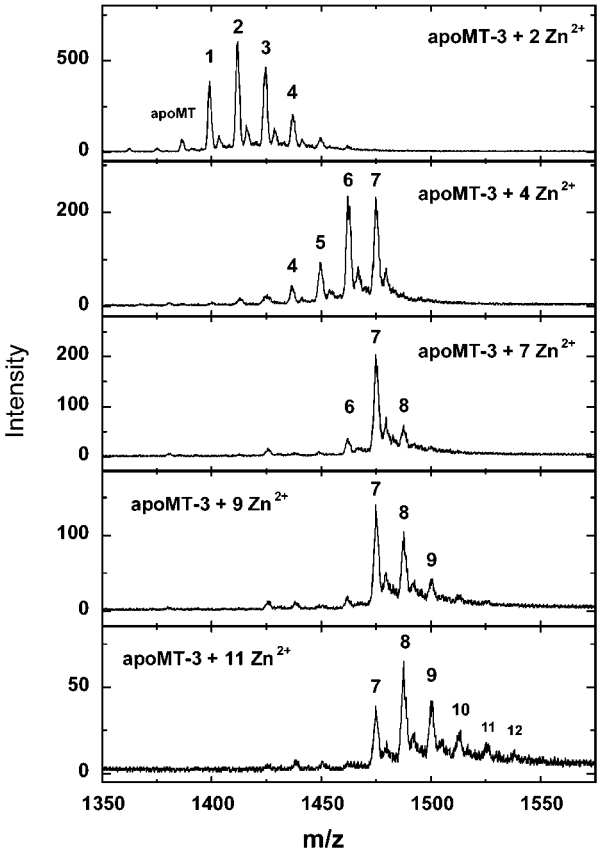

FIGURE 1: Reconstitution of apo-MT-3 (10 μM) with Zn^{2+} in 5 mM ammonium acetate (pH 7.5), containing 25 μM DTT, 25 °C. After metal addition, the samples were directly injected into the Ettan ESI-TOF-MS instrument with a flow rate of 10 μL/min and MS spectra were acquired during 2 min. Charge state +5 ions are presented and numbers on the peaks denote the metal stoichiometry of the complex.

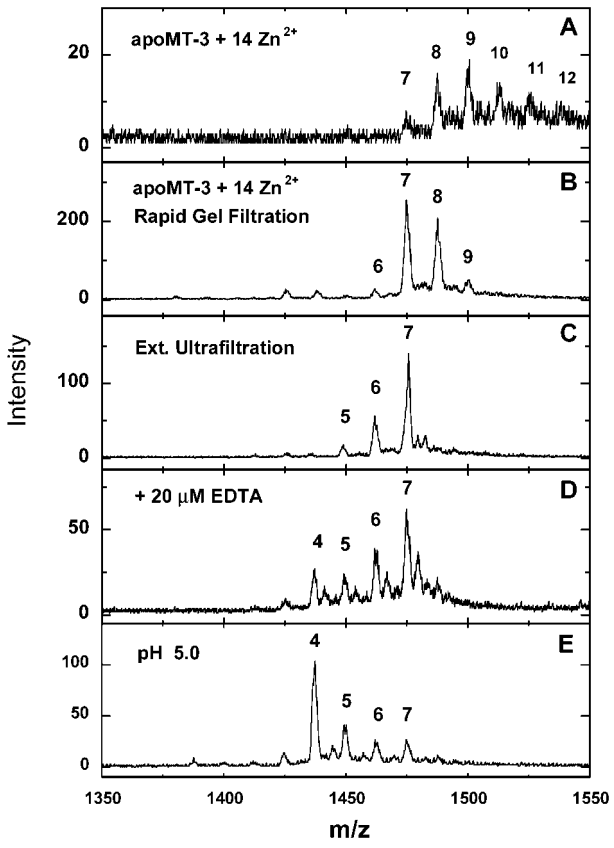

FIGURE 2: Stability of ZnMT-3. (A) ZnMT-3 (20 μM) reconstituted with 14 equiv of Zn^{2+} in 5 mM ammonium acetate (pH 7.5) and 25 μM DTT, directly infused into the MS instrument. (B) A sample as in (A), the buffer was exchanged to 5 mM ammonium acetate (pH 7.5) by fast gel filtration. (C) A sample of ZnMT-3 (10 μM, reconstituted with 7 equiv of Zn^{2+}) was concentrated 20 times by prolonged ultrafiltration (10 h), and subsequent dilution 50 times by 5 mM ammonium acetate before MS. (D) EDTA (20 μM) was added to the sample of ZnMT-3 (10 μM, reconstituted with 7 equiv of Zn^{2+}), 5 mM ammonium acetate (pH 7.5), 25 μM DTT. (E) Buffer of ZnMT-3 (10 μM, reconstituted with 8 equiv of Zn^{2+}) was exchanged to 5 mM ammonium acetate (pH 5.0) by fast gel filtration. After treatments, the samples were directly injected into an Ettan ESI-TOF-MS instrument with a flow rate of 10 μL/min and MS spectra were acquired during 2 min. Charge state +5 ions are presented and numbers on the peaks denote the metal stoichiometry of the complex.

is the one most populated. Both EDTA and pH studies indicate that a four-metal cluster exists in ZnMT-3, which is relatively more stable than other metal-binding motifs and resistant to slightly acidic conditions.

Reconstitution of MT-3 with Cd^{2+}. MS spectra of MT-3 reconstituted with increasing concentrations of Cd^{2+} at pH 7.5 are presented in Figure 3. CdMT-3, like ZnMT-3, exposes multiple metalloforms at all stoichiometries of added Cd^{2+}. MT-3 reconstituted with 7 Cd^{2+} equiv exposes four metalloforms at pH 7.5 with stoichiometries of 6−9, whereas the Cd_7MT-3 state is even less populated, as in the case of ZnMT-3. MT-3 reconstituted with 13 Cd^{2+} equiv shows a continuous spectrum of metalloforms with stoichiometries up to 12.

Stability of Cd MT-3. We tested the stability of CdMT-3 in fast gel filtration and at different pH values. The most important results are given in Figure 4. They demonstrate that CdMT-3 forms with higher metal stoichiometries than 7 are more stable in gel filtration than respective ZnMT-3 forms and are resistant to pH 5.0. At pH 3.5, CdMT-3 exposes five metalloforms with metal stoichiometries of 4−8, indicating that CdMT-3 contains a four-metal cluster, which is more stable than other metal cluster(s).

Reconstitution of MT-1 with Zn^{2+} and Cd^{2+}. MS spectra of MT-1A reconstituted with 10 equiv of Zn^{2+} and Cd^{2+} are given in Figure 5. Both Zn-MT-1A and Cd-MT-1A exist almost exclusively in the seven-metal form (Figure 5A,B). The Zn_7MT-2C form does not bind additional Zn^{2+} and is resistant to 100 μM EDTA (Figure 5C,D). Studies of the pH stability demonstrate that the three-metal cluster of MT-1 is decomposed at pH 5.0 in the case of Zn_7MT-1 (Figure 5E) and at pH 3.5 in the case of Cd_7MT-1, whereas the four-metal cluster decomposes below pH 5.0 in the case of ZnMT-1 and below pH 3.5 in the case of CdMT-1. The results obtained are in agreement with previous ESI-MS data (*23*) and with results from other spectroscopic investigations (*2*).

DISCUSSION

The results of ESI-TOF-MS experiments of MT-3 compared with common MT isoforms highlight a number of specific metal-binding properties of MT-3. The most distinctive feature of MT-3 is that this protein exists as a dynamic mixture of multiple metalloforms in solution and can adapt for binding of metals at stoichiometries lower and higher

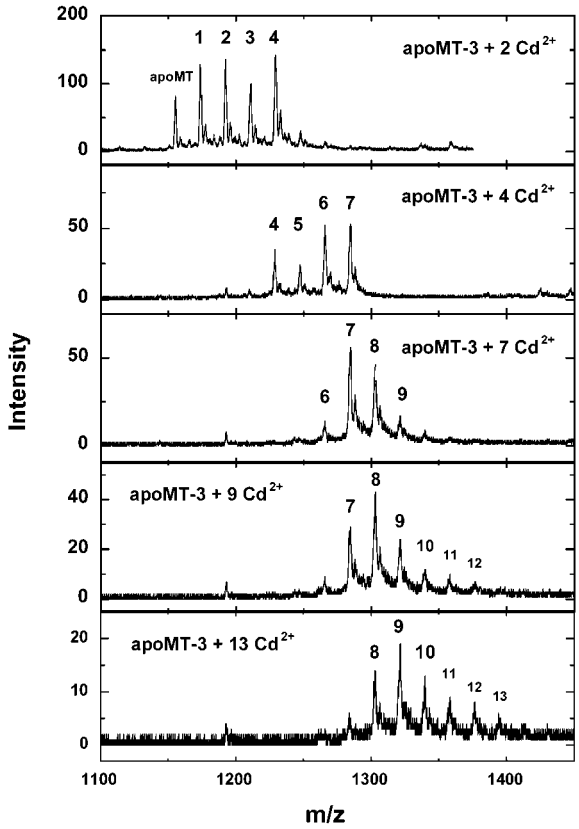

FIGURE 3: Reconstitution of apo-MT-3 (10 μM) with Cd^{2+} ions in 5 mM ammonium acetate (pH 7.5), containing 25 μM DTT, 25 °C. After metal addition, the samples were directly injected into an Ettan ESI-TOF-MS instrument at a flow rate of 10 μL/min and MS spectra were acquired during 2 min. Charge state +6 ions are presented and numbers on the peaks denote the metal stoichiometry of the complex.

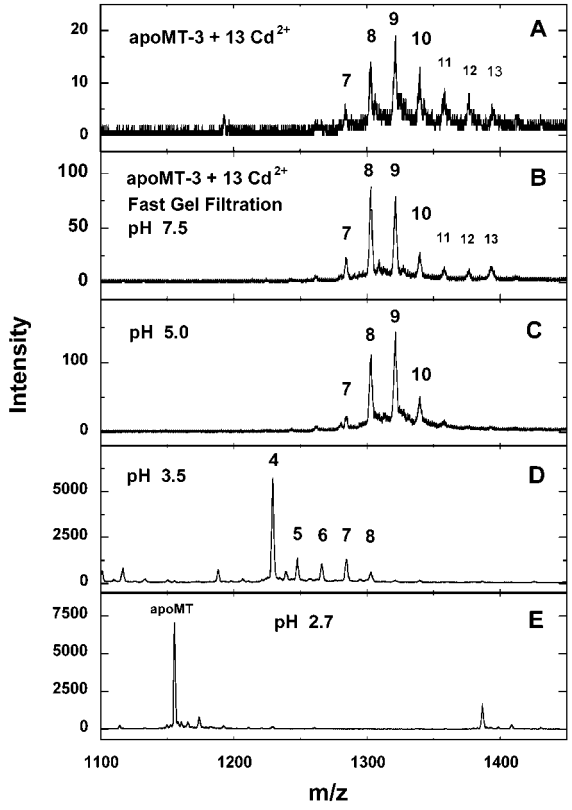

FIGURE 4: Stability of CdMT-3. (A) A sample of CdMT-3 (20 μM, reconstituted with 10 equiv of Cd^{2+}), 5 mM ammonium acetate (pH 7.5), 25 μM DTT. (B) A sample as in (A), the buffer was exchanged to 5 mM ammonium acetate (pH 7.5) by fast gel filtration. (C) As in (B), but at pH 5.0. (D) As in (B), but at pH 3.5. (E) As in (B), but at pH 2.7 (5 mM formic acid). After treatment, the samples were directly injected into the Ettan ESI-TOF-MS instrument at a flow rate of 10 μL/min and MS spectra were acquired during 2 min. Charge state +6 ions are presented and numbers on the peaks denote the metal stoichiometry of the complex.

than 7. The results of our pH studies and recent structural studies (*18*) confirm that specific metal-binding properties of MT-3 are associated largely with the N-terminal β domain of MT-3. The β domain of common MTs is adapted for cooperative binding of three divalent metal ions such as Zn^{2+} or Cd^{2+}, but binding of the same metals to the β domain of MT-3 is noncooperative as the domain can adapt a variety of metal stoichiometries. It exists in solution as a dynamic mixture of multiple metalloforms, which have similar free energies of stabilization. It is worth mentioning that all ZnMT-3 forms, even forms with sub-7 metal stoichiometries, are stable and do not tend to aggregate or oxidize even during a prolonged incubation. MT-3 metalloforms are easily interconvertible, and a metal deficit or an excess shifts the equilibria toward metalloforms with metal stoichiometries lower or higher than 7. This does not occur in the case of MT-1 or MT-2. The present results cannot specify the localization of extra metal ions in the structure of MT-3, and in principle, they may be bound to the β-cluster region, which is more disposed to structural rearrangements; however, it is not excluded that the surface carboxylates especially in the region of six-residue acidic insertion near the C-terminus of MT-3 also participate in the binding of extra metal ions.

Our results demonstrate that the β domain of MT-3 differs from the β domain of common MTs also in the stability and in the metal transfer properties. The pH studies demonstrate that the β domain of MT-3 is slightly more stable in acidic pH than the β domain of MT-1 (Figure 2E vs Figure 5E), but the experiments with EDTA demonstrate that the β domain of ZnMT-3 has a higher metal transfer potential at physiological pH than the β domain of Zn_7MT-2 (Figure 2D vs Figure 5D). Metals can be removed from the β domain of the ZnMT-3 also by ultrafiltration (Figure 2C), which indicates that there are free or low-affinity complexed metal ions present in the sample.

Reconstitution experiments with Cd^{2+} were undertaken to understand problems in structural studies of CdMT-3. The results show that CdMT-3 behaves like ZnMT-3. Only slight differences in stability of individual metalloforms were observed. Importantly, MT-3 reconstituted with 7 Cd^{2+} equiv is even more heterogeneous than ZnMT-3. Beside Cd_7MT-3, substantial amounts of metalloforms with stoichiometries 6, 8, and 9 are also observed. Thermodynamically it means that metalloforms of CdMT-3 have even closer free energies of stabilization than metalloforms of ZnMT-3. So far, the difficulties in NMR studies of CdMT-3 have been explained with conformational dynamics and fast equilibria between different conformers of the N-terminal three-metal cluster of Cd_7MT-3 (*18*−*20*). Our data demonstrate that samples of CdMT-3 are heterogeneous mixtures of different metalloforms, which are in a fast dynamic equilibrium. There may be even principal difficulties in preparation of homogeneous

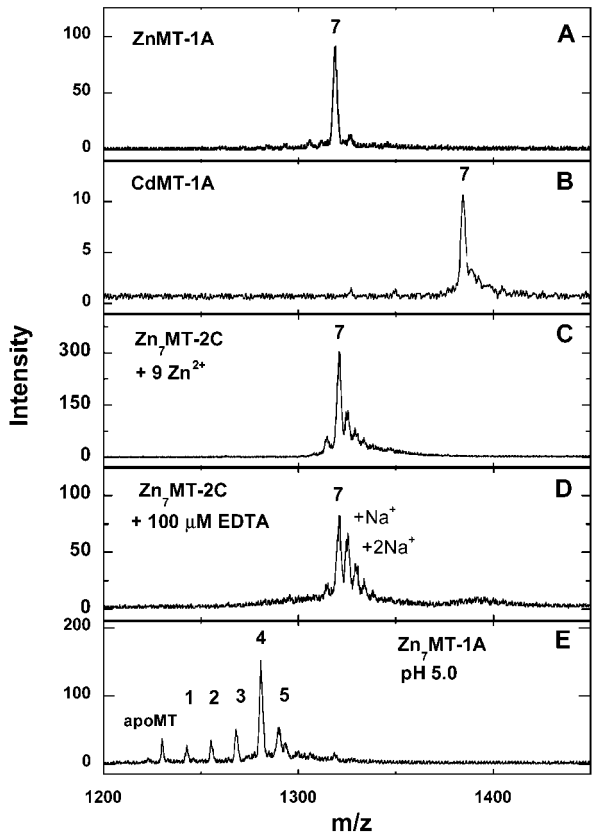

FIGURE 5: Reconstitution of MT-1 and MT-2 with Zn^{2+} and Cd^{2+} ions. (A) MT-1A (10 μM) reconstituted with 10 equiv of Zn^{2+} in 5 mM ammonium acetate (pH 7.5), 25 μM DTT. (B) MT-1A (10 μM) reconstituted with 10 equiv of Cd^{2+} in 5 mM ammonium acetate (pH 7.5), 25 μM DTT. Samples were desalted by fast gel filtration, where the buffer was exchanged to 5 mM ammonium acetate (pH 7.5). (C) Nine equivalents of Zn^{2+} were added to the sample of Zn_7MT-2C (10 μM) in 5 mM ammonium acetate (pH 7.5), 25 μM DTT. (D) EDTA (100 μM) was added to the sample of Zn_7MT-2C (10 μM) in 5 mM ammonium acetate (pH 7.5), 25 μM DTT. (E) The buffer of Zn_7MT-1A (10 μM) was exchanged to 5 mM ammonium acetate (pH 5.0) by fast gel filtration. After treatment, the samples were directly injected into the Ettan ESI-TOF-MS instrument at a flow rate of 10 μL/min and MS spectra were acquired during 2 min. Charge state +5 ions are presented and numbers on the peaks denote the metal stoichiometry of the complex.

Cd-MT-3 samples for structural studies. Therefore, heterogeneity of the sample and resulting dynamics between metalloforms could be additional reasons for reduced intensity of ^{113}Cd signals and low number of NOE signals detected from the β-cluster of CdMT-3 (*18*−*20*).

Specific metal-binding properties of MT-3 may be functionally important. They would enable MT-3 to carry out its specific physiological function. MT-3 is expressed predominantly in the brain, and MT-3 mRNA is particularly abundant in zincergic neurons, which is a subtype of glutamatergic neurons, sequestering zinc into synaptic vesicles (*15*, *25*). Transgenic experiments show that MT-3 knockout mice are normal but more sensitive to kainate-induced seizures than normal mice (*12*, *26*). As the capacity to prevent seizure activity is connected with the efficiency of zinc clearance from the synaptic cleft, it has been suggested that MT-3 may play a role in the zinc recycling process by shuttling zinc from plasma membrane to synaptic vesicles (*12*). However, up to now it was not understood how MT-3 could fulfill this function because it was thought that MT-3 is normally saturated with zinc (*12*, *16*). The present results demonstrate that even Zn_7MT-3 can bind additional zinc ions and is not saturated with the metal. Moreover, ZnMT-3 forms with sub-7 stoichiometries are also stable and can, in principle, exist in the cell. Another specific aspect of MT-3, high dynamics of Zn^{2+} exchange, favors the transfer of Zn^{2+} ions from MT-3 to the molecules participating in the transport of zinc into zinc vesicles. It is known that zinc is transported into zinc vesicles by zinc transporter ZnT-3, which is localized in the membranes of synaptic vesices (*26*). Notably, Zn-T3 knockout mice are also more susceptible to kainate-induced seizures, which gives additional support for the concept that MT-3 functions in the transfer of zinc into zinc vesicles under stimulated conditions (*27*). However, under steady-state conditions, MT-3 knockout mice expose similar levels of zinc in synaptic vesicles as in normal mice, which indicates that MT-3-mediated transport of zinc into zinc vesicles is probably duplicated also by other mechanisms (*12*). The present biochemical results demonstrate that specific metal-binding properties of MT-3 may be effectively used for buffering of highly fluctuating concentrations of zinc and transferring of zinc into synaptic vesicles in zincergic neurons.

MT-3 mRNA and the protein are significantly downregulated in the case of Alzheimer's disease (AD) (*28*). At the same time, increasing evidence demonstrates that an elevated level of free zinc could facilitate the formation of amyloid plaques characteristic for AD. In vitro experiments demonstrate that zinc can bind to amyloid β (Aβ) peptides, major constituents of amyloid plaques, and initiate their aggregation (*29*, *30*). In contrast, metal chelators can reverse aggregation of Aβ peptides and even disaggregate amyloid plaques in vivo (*31*, *32*). The listed facts support the crucial role of metals (especially zinc) in plaque formation and open a new attracting therapeutic approach in AD (*33*, *34*). Zinc-dependent plaque formation could be most critical in regions of zincergic neurons, where up to 300 μM of zinc are released into the synaptic cleft (*35*, *36*). As only 1% of this maximal zinc level can induce aggregation of Aβ peptides (*37*), slight homeostatic malfunctions in mechanisms regulating zinc metabolism may be critical for initiation or progression of amyloid plaques. Because MT-3 probably participates in buffering and uptake of free zinc in zincergic synapses, downregulation of MT-3 in AD (*28*) can lead to elevated zinc levels during neuronal stimulation, which, in turn, would promote aggregation of Aβ peptides and progression of AD pathology.

ACKNOWLEDGMENT

The authors thank Professor R. Palmiter for the donation of cDNA, Amersham Biosciences for support and Staffan Renlund and Henrik Wadensten for assistance.

REFERENCES

1. Binz, B. A., and Kägi, J. H. R. (1999) in *Metallothionein IV* (Klaassen, J., Ed.), pp 7−13, Birkhäuser, Basel, Switzerland.
2. Vašák, M., and Kägi, J. H. R. (1994) in *Encyclopedia of Inorganic Chemistry* (King, R. B., Ed.), pp 2229−2241, John Wiley and Sons Ltd., New York.
3. Davis, S. R., and Cousins, R. J. (2000) *J. Nutr. 130*, 1085−1088.
4. Frey, M. H., Wagner, G., Vašák, M., Sorensen, O. W., Neuhaus, D., Worgotter, E., Kägi, J. H. R., Ernst, R. R., and Wüthrich, K. (1985) *J. Am. Chem. Soc. 107*, 6847−6851.

5. Robbins, A. H., McRee, D. E., Williamson, M., Collett, S. A., Xuong, N. H., Furey, W. F., Wang, B. C., and Stout, C. D. (1991) *J. Mol. Biol. 221*, 1269−1993.
6. Braun, W., Vašák, M., Robbins, A. H., Stout, C. D., Wagner, G., Kägi, J. H. R., and Wüthrich, K. (1992) *Proc. Natl. Acad. Sci. U.S.A. 89*, 10124−10128.
7. Uchida, Y., Takio, K., Titani, K., Ihara, Y., and Tomonaga, M. (1991) *Neuron 7*, 337−347.
8. Palmiter, R. D., Findley, S. D., Whitmore, T. E., and Durnam, D. M. (1992) *Proc. Natl. Acad. Sci. U.S.A. 89*, 6333−6337.
9. Zheng, H., Berman, N. E. J., and Klassen, C. D. (1995) *Neurochem. Int. 27*, 43−58.
10. Kobayashi, H., Uchida, Y., Ihara, Y., Nakajima, K., Kohsaka, S., Miyatake, T., and Tsuji, S. (1993) *Mol. Brain Res. 19*, 188−194.
11. Erickson, J. C., Masters, B. A., Ba Kelly, E. J., Brinster, R. I., and Palmiter, R. D. (1995) *Neurochem. Int. 27*, 35−41.
12. Erickson, J. C., Hollopeter, G., Thomas, S. A., Froelick, G. J., and Palmiter, R. D. (1997) *J. Neurosci. 17*, 1271−1281.
13. Erickson, J. C., Sewell, A. K., Jensen, L. T., Winge, D. R., and Palmiter, R. D. (1994) *Brain Res. 649*, 297−304.
14. Sewell, A. K., Jensen, L. T., Erickson, J. C., Palmiter, R. D., and Winge, D. R. (1995) *Biochemistry 34*, 4740−4747.
15. Masters, B. A., Quaife, C. J., Erickson, J. C., Kelly, E. J., Froelick, G. J., Zambrowicz, B. P., Brinster, R. L., and Palmiter, R. D. (1994) *J. Neurosci. 14*, 5844−5857.
16. Aschner, M., Cherian, M. G., Klaassen, C. D., Palmiter, R. D., Erickson, J. C., and Bush, A. I. (1997) *Toxicol. Appl. Pharmacol. 142*, 229−242.
17. Vašák, M., Hasler, D. W., and Faller, P. (2000) *J. Inorg. Biochem. 79*, 7−10.
18. Öz, G., Zangger, K., and Armitage, I. M. (2001) *Biochemistry 40*, 11433−11441.
19. Hasler, D. W., Jensen, L. T., Zerbe, O., Winge, D. R., and Vašák, M. (2000) *Biochemistry 39*, 14567−14575.
20. Faller, P., Hasler, D. W., Zerbe, O., Klauser, S., Winge, D. R., and Vasak, M. (1999) *Biochemistry 38*, 10158−10167.
21. Vašák, M. (1991) *Methods Enzymol. 205*, 41−44.
22. Hunziker, P. E., Kaur, P., Wan, M., and Kanzig, A. (1995) *Biochem. J. 306*, 265−270.
23. Gehrig, P. M., You, C. H., Dallinger, R., Gruber, C., Brouwer, M., Kagi, J. H. R., and Hunziker, P. E. (2000) *Protein Sci. 9*, 395−402.
24. Vašák, M. (1991) *Methods Enzymol. 205*, 452−458.
25. Frederickson, C. J., Suh, S. W., Silva, D., and Thompson, R. B. (2000) *J. Nutr. 130*, 1471S−1483S.
26. Wenzel, H. J., Cole, T. B., Born, D. E., Schwartzkroin, P. A., and Palmiter, R. D. (1997) *Proc. Natl. Acad. Sci. U.S.A. 94*, 12676−12681.
27. Cole, T. B., Robbins, C. A., Wenzel, H. J., Schwartzkroin, P. A., and Palmiter, R. D. (2000) *Epilepsy Res. 39*, 153−169.
28. Yu, W. H., Lukiw, W. J., Bergeron, C., Niznik, H. B., and Fraser, P. E. (2001) *Brain Res. 894*, 37−45.
29. Mantyh, P. W., Ghilardi, J. R., Rogers, S., DeMaster, E., Allen, C. J., Stimson, E. R., and Maggio, J. E. (1993) *J. Neurochem. 61*, 1171−1174.
30. Bush, A. I., Pettingell, W. H., Multhaup, G., d Paradis, M., Vonsattel, J. P., Gusella, J. F., Beyreuther, K., Masters, C. L., and Tanzi, R. E. (1994) *Science 265*, 1464−1467.
31. Cherny, R. A., Atwood, C. S., Xilinas, M. E., Gray, D. N., Jones, W. D., McLean, C. A., Barnham, K. J., Volitakis, I., Fraser, F. W., Kim, Y., Huang, X., Goldstein, L. E., Moir, R. D., Lim, J. T., Beyreuther, K., Zheng, H., Tanzi, R. E., Masters, C. L., and Bush, A. I. (2001) *Neuron 30*, 665−676.
32. Gouras, G. K., and Beal, M. F. (2001) *Neuron 30*, 641−642.
33. Cherny, R. A., Barnham, K. J., Lynch, T., Volitakis, I., Li, Q. X., McLean, C. A., Multhaup, G., Beyreuther, K., Tanzi, R. E., Masters, C. L., and Bush, A. I. (2000) *J. Struct. Biol. 130*, 209−216.
34. Cuajungco, M. P., Faget, K. Y., Huang, X., Tanzi, R. E., and Bush, A. I. (2000) *Ann. N. Y. Acad. Sci. 920*, 292−304.
35. Assaf, S. Y., and Chung, S. H. (1984) *Nature 308*, 734−736.
36. Howell, G. A., Welch, M. G., and Frederickson, C. J. (1984) *Nature 308*, 736−738.
37. Huang, X., Cuajungco, M. P., Atwood, C. S., Moir, R. D., Tanzi, R. E., and Bush, A. I. (2000) *J. Nutr. 130*, 1488S−1492S.

BI025664V